Neurobiology of Disease 48 (2012) 309–316

Contents lists available at SciVerse ScienceDirect

Neurobiology of Disease

journal homepage: www.elsevier.com/locate/ynbdi

Spatiotemporal evolution of blood brain barrier damage and tissue infarction within the first 3 h after ischemia onset

Xinchun Jin [a,1,2], Jie Liu [a,1], Yi Yang [b], Ke J. Liu [a,b], Yirong Yang [a], Wenlan Liu [a,*]

[a] College of Pharmacy, University of New Mexico Health Sciences Center, Albuquerque, NM 87131, USA
[b] Department of Neurology, University of New Mexico Health Sciences Center, Albuquerque, NM 87131, USA

ARTICLE INFO

Article history:
Received 16 March 2012
Revised 29 June 2012
Accepted 9 July 2012
Available online 17 July 2012

Keywords:
Blood brain barrier
Cerebral ischemia
Matrix metalloproteinases
Tissue infarction

ABSTRACT

Blood brain barrier (BBB) damage that occurs within the thrombolytic time window is increasingly appreciated to negatively impact the safety and efficacy profiles of thrombolytic therapy for ischemic stroke. However, the spatiotemporal evolution of BBB damage in this early stroke stage and the underlying mechanisms remain unclear. Here, we investigated the topographical distribution of BBB damage and its association with tissue injury within the first 3 h after ischemia onset and the roles of matrix metalloproteinase (MMP)-2/9 in this process. Rats were subjected to 1, 2, or 3 h of middle cerebral artery occlusion (MCAO) followed by 10 min reperfusion with fluorescence-labeled dextran as BBB permeability marker. Acute tissue infarction was evidenced by staining defect with triphenyltetrazolium chloride (TTC). Cerebral blood flow (CBF) was measured by magnetic resonance imaging. MMP-2/9 were assessed by gel and *in situ* zymography. After 2-h MCAO, dextran leakage was seen in the ischemic ventromedial striatum and the preoptic area which showed ~70% CBF reduction, and expanded to other MCA regions including the cortex after 3-h MCAO. Interestingly, high (2000 kDa) and low (70 kDa) molecular weight dextrans displayed almost identical leakage patterns. Different from BBB damage, tissue infarction was first seen in the ischemic dorsal striatum and the parietal/insular cortex which experienced ~90% CBF reduction. Increased gelatinolytic activity colocalized with dextran leakage, and MMP-2 was found to be the major enzymatic source on gelatin zymograms. Pretreatment with MMP inhibitor GM6001 significantly reduced dextran leakage induced by 2-h and 3-h MCAO. Taken together, our findings reveal substantial differences in the topographic distribution of BBB damage and tissue infarction within the first 3 h after MCAO onset. Unlike ischemic neuronal damage, BBB damage appears to develop faster in brain regions with moderately severe ischemia, and MMP-2 contributes to this early ischemic BBB damage.

Introduction

Ischemic stroke results from acute arterial occlusion leading to focal hypoperfusion. Thrombolysis remains the only proven treatment. While the presence of a salvageable penumbra has been widely agreed as the premise for thrombolytic therapy (Foley et al., 2010), the status of the blood brain barrier (BBB) integrity at thrombolytic intervention is considered to be central to the risks of vasogenic edema and hemorrhagic transformation (del Zoppo et al., 1998). In a clinical magnetic resonance imaging (MRI) study, Warach and Latour (2004) reported that 8 out of 9 stroke patients who had early ischemic BBB damage underwent cerebral bleeding and showed worse outcome following thrombolytic therapy. Several more recent animal and human studies found that thrombolysis-associated cerebral hemorrhage occurred in the brain regions where the BBB was compromised at a much earlier stroke stage (Bang et al., 2007; Hjort et al., 2008; Hom et al., 2011; Kassner et al., 2009; Sun et al., 2010; Wu et al., 2009). These studies suggest that loss of BBB integrity during cerebral ischemia may predispose ischemic brain tissue to bleeding during thrombolytic reperfusion, thus underscoring a pivotal role of early ischemic BBB in thrombolytic therapy. However, how the BBB is damaged during acute cerebral ischemia, particularly within the 3-h thrombolytic time window, remains to be elucidated.

BBB damage during postischemic reperfusion has been extensively studied, which occurs as the result of oxidative damage due to increased free radical generation (Liu and Rosenberg, 2005), proteolytic degradation by matrix metalloproteinases (MMPs) (Yang et al., 2010) and inflammatory activation (Tomita and Fukuuchi, 1996). In addition, depending on the methodology used, several earlier studies reported

Abbreviations: BBB, blood brain barrier; CBF, cerebral blood flow; MCAO, middle cerebral artery occlusion; MMP, matrix metalloproteinase; tPA, tissue plasminogen activator; MRI, magnetic resonance imaging; TTC, 2,3,5-triphenyltetrazolium chloride; FITC, fluorescein isothiocyanate-conjugated dextran; ROI, region of interest.

* Corresponding author. Fax: +1 505 272 0704.
E-mail address: weliu@salud.unm.edu (W. Liu).

Available online on ScienceDirect (www.sciencedirect.com).

[1] Both authors contributed equally to this work.

[2] Present address: Department of Neuroscience, Georgetown University, Washington, DC 20057, USA.

0969-9961/$ – see front matter © 2012 Elsevier Inc. All rights reserved.
doi:10.1016/j.nbd.2012.07.007

a biphasic pattern of BBB opening during reperfusion (Belayev et al., 1996; Huang et al., 1999; Kuroiwa et al., 1985), while a more recent study reported continuous BBB opening for several weeks (Strbian et al., 2008). There are a few studies that were in attempt to explore BBB damage at relatively early stroke stages using animal stroke models of up to 4-h cerebral ischemia followed by 20 min to 3 h of reperfusion, but obtained quite inconsistent or even contradictory results. For example, Gerriets et al. (2009) observed Evans blue extravasation in the ischemic brain following 20 min cerebral ischemia plus 20 min reperfusion, DiNapoli et al. (2008) showed dextran extravasation in young and aged rats after 2 h cerebral ischemia with 20 min reperfusion, and Chen et al. (2009) reported BBB leakage after 1 h cerebral ischemia plus 30 min reperfusion. These reports are contradicted by earlier findings that tracer extravasation was not detectable earlier than a few hours (≥4 h) after vessel occlusions (Belayev et al., 1996; Betz and Coester, 1990; Menzies et al., 1993). To our best knowledge, no studies have specifically designed to characterize ischemic BBB damage that occurs within the 3-h thrombolytic time window including topographic distribution, temporal evolution, size of opening, and its association with ischemic tissue injury.

In a recent study, we showed that the BBB was disrupted *in vitro* and *in vivo* after 2-h ischemia, and in the *in vitro* cellular experiments, we demonstrated that caveolin-1-mediated claudin-5 redistribution and MMP-2-mediated occludin degradation accounted for rapid endothelial barrier disruption induced oxygen-glucose deprivation (Liu et al., 2012). In this study, we continued our investigation of early ischemic BBB damage using the rat model of middle cerebral artery occlusion (MCAO) by investigating the spatiotemporal evolution of ischemia-induced BBB damage and its relation to brain tissue infarction within the first 3 h after MCAO onset. Moreover, we investigated the early changes of the gelatinases MMP-2/9 in the ischemic brain tissue and their role in early ischemic damage *in vivo*.

Materials and methods

Animal model of focal cerebral ischemia

The Laboratory Animal Care and Use Committee at the University of New Mexico approved all experimental protocols. Male Sprague–Dawley rats (Charles River) weighing 290 to 325 g were subjected to 1, 2, or 3 h of MCAO followed by 10 min of reperfusion using the intraluminal suture occlusion model, as we described previously (Liu et al., 2009b). Rats were anesthetized with 2% isoflurane during surgical procedures. Prior to reperfusion, all rats included in this study (n = 106) displayed neurologic deficit typical of MCAO, circling to the left (non-ischemic side). Detailed animal usage for each experiment was listed in the figures or figure legends. For the majority of 2-h and 3-h MCAO rats, successful MCAO was further confirmed by 2,3,5-triphenyltetrazolium chloride (TTC) staining. Seven rats were excluded from this study due to insufficient arterial occlusion reflected by not circling to the left at the end of ischemia. No rats died because of stroke or surgical complications.

Experimental design and tissue processing

The study consisted of two different experiments: Experiment 1 aimed to evaluate the spatiotemporal evolution of ischemic BBB damage and tissue infarction within the first 3 h after ischemia onset. BBB damage was determined by assessing the extravasation of fluorescein isothiocyanate-conjugated dextran (FITC-dextran, 2000 kDa, Sigma, St Louis, MO, USA). Immediately after MCAO, 0.3 ml of 5% FITC-dextran (wt/vol in sterile PBS) was injected through the left femoral vein. All rats were reperfused for 10 min to allow sufficient circulation of FITC-dextran to the ischemic brain, but minimize the impact of reperfusion on BBB integrity. At the end of reperfusion, the rats were transcardially perfused with ice-cold PBS and then the brain was quickly taken out. A 5-mm-thick brain region approximately spanning from +1.5 to −3.5 mm relative to the bregma was quickly cut, frozen in pre-chilled (−80 °C) 2-methylbutane, and embedded in OCT solution for cryosectioning. The selection of this particular region was based on our initial observation that FITC-dextran leakage in 3-h MCAO rats occurred in the ischemic brain extending from approximately +1.0 to −3.0 mm relative to the bregma. A set of 10 consecutive 20-μm-thick brain sections was generated from the selected brain region at 450 μm interval along the rostrocaudal axis on a Leica cryostat (Leica, Microsystems Inc., Buffalo Grove, IL, USA). Each section was photographed under Olympus IX-81 microscope with Stereo Investigator software (Olympus, Optical Co. Ltd, Japan) to visualize the location and size of FITC-dextran leakage. Besides characterizing the topographic distribution of FITC-dextran leakage, the mean leakage area was calculated as averaged area proportion of the sections measured.

Tissue infarction in terms of location and size was assessed by TTC staining of 1-mm-thick brain slice (Liu et al., 2008). Under our experimental condition, appreciable tissue infarction (or TTC staining defect) was found to be visible within an 8-mm-thick brain region extending approximately from +3.5 to −4.5 mm relative to the bregma. To allow for a more direct comparison of spatial distribution between early BBB damage and tissue infarction, rats were subjected to 2-h MCAO, and FITC-dextran leakage and tissue infarction were compared on the same 2-mm-thick brain slices that were sectioned out at the level immediately after the bregma.

The high molecular weight (2000 kDa) FITC-dextran may only label tissue with severe BBB damage (Chen et al., 2009), and an upper size limit for this tracer was reported following 3-h MCAO with 3 h of reperfusion (Nagaraja et al., 2008). To determine whether early ischemic BBB opening has a similar upper size-limit or presents as "all-or-none" phenomenon, a mixture of FITC-dextran (2000 kDa) and Texas red-dextran (70 kDa, Sigma) was injected to rats at the end of 2-h MCAO. Three consecutive 20-μm-thick brain cryosections (starting at around the bregma level) at 600 μm interval along the rostrocaudal axis were prepared and photographed to compare the leakage between these two tracers.

In Experiment 2, we assessed the changes of MMP-2/9 and their roles in early ischemic BBB damage. All the following measurements were focused on the 2-mm-thick brain region extending from 0.0 to −2.0 mm relative to the bregma because this region showed the biggest FITC-dextran leakage (in terms of fluorescent intensity and leakage size) in Experiment 1 for both 2-h and 3-h MCAO rats, and could thus represent the central slice of the MCA territory. MMP-2/9 were assessed by gel and *in situ* zymography, as described in more detail later. For *in situ* zymography, FITC-dextran was replaced by Rhodamine-conjugated dextran (2000 kDa, Invitrogen, Carlsbad, CA, USA) because the cleavage of FITC-labeled DQ-gelatin by MMP-2/9 yields green fluorescence. To establish a causal role of MMP-2/9 in early ischemic BBB damage, the broad spectrum MMP inhibitor GM6001 or its negative control (10 μg/kg in 5 μl DMSO, EMD Biosciences, La Jolla, CA, USA) was given to rats *via* the carotid artery 10 min before MCAO, and FITC-dextran leakage area was quantified on the 20-μm-thick brain section (at ~−1.0 mm relative to the bregma). To confirm successful MCAO, one 1-mm-thick brain slice right before the "central slice" was cut for TTC staining. We only tested the effects of GM6001 on 2-h and 3-h MCAO rats because no tracer leakage was observed for 1-h MCAO rats in Experiment 1.

Gel gelatin zymography

Ischemic and nonischemic hemispheric tissues collected from the central slice as described above were homogenized in MMP lysis buffer, and MMP-2/9 levels in homogenates were assessed by gel gelatin zymography as we described previously (Yang et al., 2007). A mixture of human MMP-2/9 (Invitrogen) was used as gelatinase standards.

In situ zymography

The gelatinolytic activity of MMP-2/9 in brain tissue injected with Rhodamine-conjugated dextran was analyzed by *in situ* zymography using EnzCheck Collagenase Kit (EnzCheck Collagenase Kit, Invitrogen) following the manufacturer's instructions. The 20-μm-thick cryosections sampled from the central slice were incubated in a humidity chamber for 1 h at 37 °C in a reaction buffer containing 30 μg/ml of FITC-labeled DQ-gelatin. Sections were rinsed and mounted for fluorescent microscopic observation. BBB disruption was reflected by Rhodamine-dextran extravasation (red), and the gelatin-FITC is cleaved by gelatinases, yielding peptides whose fluorescence is representative of net proteolytic activity (green).

CBF measurements with MRI

In Experiment 1, we observed an unexpected phenomenon that BBB damage did not overlap well with tissue infarction (or TTC staining defect) after 2-h MCAO. To further confirm whether TTC staining defect was due to severe cerebral blood flow (CBF) reduction, estimates of CBF were acquired 105–120 min after MCAO onset using an arterial spin labeling technique (Williams et al., 1992). MRI studies were performed on a 4.7-Tesla, 40-cm bore Bruker AVANCE system (Billerica, MA, USA), equipped with 500 mT/m (rise time 80–120 μs) gradient set and a small bore linear RF coil (ID 72 mm). The CBF estimates were acquired using the IR RARE sequence with TR/TE = 10,000/46 ms, 128×128 matrix, 32×32 mm FOV. The 1-mm-thick image slice was located approximately −1.0 mm relative to the bregma. CBF maps were calculated by ASL_Perfusion_Processing Macro in Paravision 5.1 (Bruker) and four regions of interest (ROIs) were placed manually on the CBF maps as shown in Fig. 3A. All 4 ROIs were mirrored to the nonischemic hemisphere. The ratios between physiological estimates of the lesion and of the contralateral mirror ROI were then determined.

Statistical analysis

The data are presented as mean ± SEM. Statistical analysis was carried out using ANOVA (three or more groups) or student *t* test (two groups) (SPSS software, version 17.0). Significant effects were probed using Newman–Keuls *post hoc* comparison. A value of $P<0.05$ was considered statistically significant.

Results

Spatiotemporal evolution of BBB damage and tissue infarction within the first 3 h after ischemia onset

Fluorescent micrographs showed topographic distribution of BBB damage 1, 2, and 3 h after MCAO (Fig. 1A). Two-hour MCAO, but not 1-h MCAO, induced dextran leakage in the ventromedial striatum and the preoptic area of the ischemic hemisphere. After 3-h MCAO, dextran leakage expanded to more subcortical tissue along the rostrocaudal axis, and half of the rats showed spotted dextran leakage in the ischemic cortex. No dextran leakage was observed in the nonischemic hemisphere of all tested rats. Worthy of note, dextran leakage appeared to peak at the 2-mm-thick brain region extending from approximately 0.0 to −2.0 mm relative to the bregma for both 2-h and 3-h MCAO rats, which probably represents the central slice of the MCA territory and was thus chosen to examine the changes of MMP-2/9 later in this study.

Similar to BBB damage, tissue infarction reflected by TTC staining defect, was not appreciable in 1-h MCAO rats, but was clearly seen after 2 or 3 h of MCAO (Fig. 1B). To our surprise, the topographic distribution of tissue infarction was very different from that of BBB damage, in which tissue infarction was first seen in the dorsolateral striatum and parietal/insular cortex (2 h after MCAO) and expanded to most of the MCA-supplied territory after 3-h MCAO (Fig. 1B). The size of the infarct area was significantly greater than that of the tracer leakage area for both 2-h (9.38 ± 0.89% *versus* 3.62 ± 0.24%, $P<0.05$) and 3-h (16.12 ± 0.60% *versus* 7.70 ± 0.74%, $P<0.05$) MCAO rats (Fig. 1C).

To more directly compare the patterns of tissue lesion and BBB damage, the 2-mm-thick central slice obtained from 2-h MCAO rats was first subjected to TTC staining and then cryosectioned after fixation to visualize BBB leakage. Clearly, there was almost no co-localization of tissue infarction and BBB leakage on the same brain slice (Fig. 1D).

Size of early ischemic BBB opening

An upper size limit for the extravasation of 2000 kDa FITC-dextran was reported following 3-h MCAO with 3 h of reperfusion (Nagaraja et al., 2008). To determine whether there is a similar upper size of BBB opening resulting from early ischemia, a mixture of FITC-dextran (2000 kDa, high molecular weight) and Texas red-dextran (70 kDa, low molecular weight) was injected to the rats after 2-h MCAO, and their leakage was compared on three consecutive cryosections (Fig. 2A). To our surprise, the leakage of high and low molecular dextrans occurred in the same locations, *i.e.* the ventromedial striatum and preoptic area (Fig. 2B). On each section, the leakage area for high and low molecular dextrans showed more than 96% overlap, with a slight larger leakage area for low dextran (Fig. 2C). Similar to 2000 kDa dextran, we did not observe any leakage of 70 kDa dextran in 1-h MCAO rats (data not shown).

CBF changes in the regions of interest

CBF reductions in the parietal/insular cortex (ROI 1), dorsolateral striatum (ROI 2), ventromedial striatum (ROI 3) and preoptic area (ROI 4) were measured with MRI. In all five rats, the CBF maps showed reduced CBF in the MCA-supplied territory of the ischemic hemisphere (Fig. 3A). The ratios of CBF between ischemic ROIs and their mirrored ROIs on the nonischemic hemisphere revealed that CBF reduction in ROIs 1 and 2 was more severe (~90%) than that (~70%) in ROIs 3 and 4 (Fig. 3B), which was in line with our observation of a higher susceptibility of brain tissue in ROIs 1 and 2 to ischemic injury (Fig. 1B). Surprisingly, ischemic BBB damage (Fig. 1A) appeared to first occur in ischemic tissue (ROIs 3 and 4) with less severe CBF reduction.

MMP-2 contributes to early ischemic BBB damage

MMP-2/9 levels were analyzed with gel zymography after 1, 2 and 3 h of MCAO (Fig. 4A). As expected, the levels of both MMPs were comparable in the nonischemic tissue across all three ischemic conditions (Fig. 4B). For the 1-h MCAO rats, no significant difference was observed for both MMPs between ischemic and nonischemic tissues (Fig. 4B). A significant increase in MMP-2 levels was detected after 2-h MCAO, which was not further increased after MCAO duration was prolonged to 3 h (Fig. 4C). Comparing to MMP-2, MMP-9 was expressed at a much lower level and responded to cerebral ischemia in a slightly delayed pace, in which a significant increase in MMP-9 was induced only after 3-h MCAO (Fig. 4D).

In situ zymography was performed to determine the spatial locality of gelatinase activation and its colocalization with early BBB damage induced by 2-h MCAO (Fig. 5A). Rhodamine-dextran leakage was clearly seen in the ischemic preoptic area (Fig. 5B), confirming the results we showed earlier in Fig. 1A. After incubating with FITC-labeled DQ gelatin, increased gelatinolytic activity (green fluorescence) was seen in the ischemic preoptic area where dextran leakage occurred, when comparing with the low basal gelatinolytic activity nonischemic hemispheric

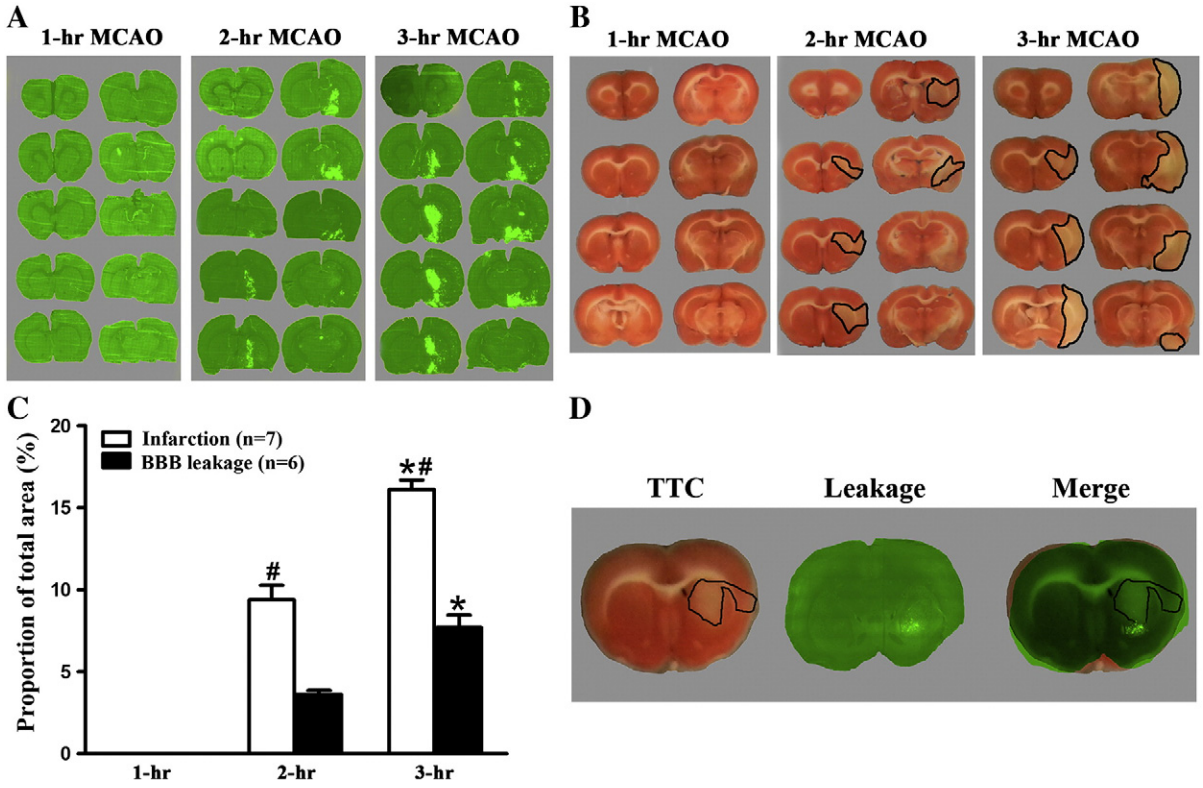

Fig. 1. Evolution of BBB damage and tissue infarction within the first 3 h after MCAO onset. A, Representative fluorescent microscopic images of consecutive cryosections showing FITC-dextran leakage (bright green) in the ischemic hemisphere. Dextran leakage was limited to the ischemic ventromedial striatum and preoptic area after 2-h MCAO, which spread to more ischemic subcortical tissue and the ischemic cortex after 3-h MCAO. No tracer leakage was observed for 1-h MCAO rats. B, Representative TTC-stained brain slices showing staining defects or tissue infarction, which was tagged by black closed line. After 2-h MCAO, tissue infarction was seen in the ischemic dorsolateral striatum and the parietal/insular cortex, which spread to the majority of MCA-supplied territory at 3-h MCAO. No appreciable TTC staining defects were observed for the 1-h MCAO rats. C, The dextran leakage and tissue infarction were quantified and expressed as averaged area proportion of the sections measured (%). Three-hour MCAO rats showed larger affected area with tissue infarction and BBB damage than 2-h MCAO rats ($^{*}P<0.05$ *versus* 2-h MCAO). The infarct size was significantly larger than BBB leakage size for both 2-h and 3-h ischemic durations ($^{\#}P<0.05$ *versus* BBB leakage). Data were expressed as mean ± SEM. D, Representative images showing that BBB leakage (Middle) did not occur within the infarct after 2-h MCAO (left), which was more clearly revealed in the merged image (right). N = 4 for this experiment. Note: two images did not merge perfectly due to post-processing after TTC staining such as fixation and freezing. (For interpretation of the references to color in this figure legend, the reader is referred to the web version of this article.)

tissue. Remarkably, some increased gelatinolytic activities were found to be prominent along with the leaky ischemic microvessels (Fig. 5B).

To establish a causative role of MMP-2/9 in early ischemic BBB damage, MMP inhibitor GM6001 or its negative control was administered to rats 10 min before MCAO. As shown in Fig. 6, GM6001 significantly reduced dextran leakage area after 2 h-MCAO (10.35 ± 1.79% *versus* 2.03 ± 1.29%, $P<0.05$) or 3-h MCAO (40.41 ± 6.79% *versus* 7.99 ± 2.74%, $P<0.05$), when compared to its negative control (Control). Consistent with what we observed earlier in Fig. 1D, tissue infarction did not co-localize well with FITC-dextran leakage (Figs. 6A and C). Although we did not quantify the infarcted area of TTC-stained slices, GM60001 seemed to have no significant effect on tissue infarction.

Discussion

Thrombolytic reperfusion with tPA remains the only FDA-approved stroke therapy, and its efficacy largely relies on the presence of considerable amount of salvageable penumbral tissue (Foley et al., 2010) and the tightness of the BBB at thrombolytic intervention (Benchenane et al., 2005a,2005b; Qin et al., 2007). Thus, understanding the spatiotemporal profiles of early ischemic injuries to neuronal tissue and the BBB is essential for maximizing therapeutic effect while avoiding the potentially devastating neurovascular complications associated with reperfusion. Here, we investigated the spatiotemporal pattern of ischemic BBB damage and its association with tissue infarction within the established 3-h thrombolytic time window. Our important findings include: (1) 2- and 3-h, but not 1-h MCAO, induced appreciable tissue infarction and BBB damage, (2) BBB damage was first seen in the ischemic ventromedial striatum and the preoptic area, which experienced approximately 70% reduction in CBF, while tissue infarction occurred first in the dorsal striatum and the parietal/insular cortex where CBF reduction was more profound (~90% reduction), and (3) the gelatinases, particularly MMP-2, were implicated in early ischemic BBB damage.

Using fluorescence-labeled tracer and TTC staining, we characterized the topographic distribution of early ischemic BBB damage and tissue infarction. Under our experimental condition, 1-h MCAO did not induce appreciable BBB damage and tissue infarction, so the discussion below, if not specifically stated, is on 2- and 3-h MCAO. For both MCAO durations, a significantly larger volume was observed for tissue infarction than BBB damage. This is in line with the general belief that the neuronal tissue is more susceptible to ischemic insult than the cerebro-microvasculature (Dewar et al., 2003; Namura et al., 1998). Interestingly, BBB damage was first seen in the ventromedial striatum and the preoptic area, while tissue infarction first occurred in the dorsal striatum and the parietal/insular cortex after MCAO. As a consequence, an unexpected topographic "mismatch" between BBB damage and tissue infarction is consistently seen in the ischemic hemisphere after 2-h MCAO. Although TTC staining defect reliably reflects irreversible tissue injury (Bederson et al., 1986; Vivaldi et al., 1985), it is possible that, at such an early time after MCAO onset, some ischemic tissue positively stained with TTC may be in the middle of the dying process stage, but the damage is already irreversible. Therefore, TTC staining defect may not be able to accurately demarcate all the areas with irreversibly injured tissue at 2 h

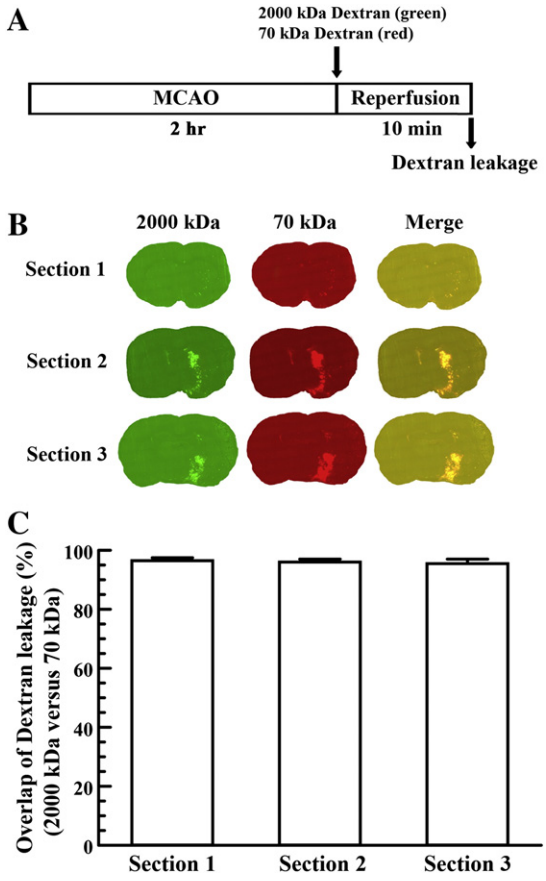

Fig. 2. 2000 kDa and 70 kDa dextrans showed almost identical pattern of extravasation after 2-h MCAO. A, Diagram of the experimental procedure. B, Representative fluorescent micrographs of three consecutive brain sections (starting at around the bregma level) at 600 μm interval along the rostrocaudal axis showed good colocalization for the extravasation of both tracers in ischemic ventromedial striatal and preoptic area. C, The overlapped leakage on each section was quantified *via* dividing the leakage area of 70 kDa dextran by that of 2000 kDa dextran and expressed as percentage. A greater than 96% overlap of tracer leakage was observed on each section, with a slight larger leakage for 70 kDa dextran. Data were expressed as mean ± SEM, n = 4.

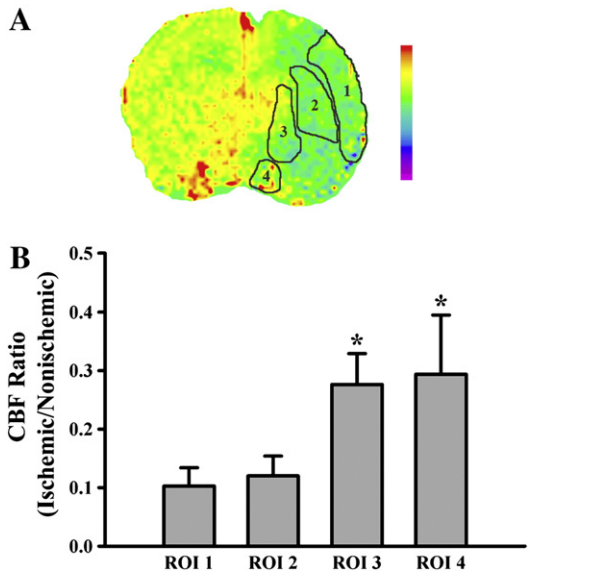

Fig. 3. Perfusion-weighted imaging with MRI showed heterogeneous CBF changes in the regions of interest after MCAO. Perfusion map was acquired at 105 to 120 min after MCAO onset. A, CBF was greatly lowered in the MCA territory of the ischemic hemisphere (purple, blue and dark green pixels). Color scale for CBF: purple-to-red: minimum-to-maximum. B, Ratios of CBF (ischemic/nonischemic) were quantified in the parietal/insular cortex (ROI 1), dorsolateral striatum (ROI 2), ventromedial striatum (ROI 3), and preoptic area (ROI 4) (marked in A as numbers 1, 2, 3, and 4, respectively). After approximately 2-h MCAO, CBF reduction in ROIs 1 and 2 was more severe than that in ROIs 3 and 4, Data were expressed as mean ± SEM, $^{*}P<0.05$ *versus* ROIs 1 and 2, n = 5. (For interpretation of the references to color in this figure legend, the reader is referred to the web version of this article.)

after MCAO. To overcome this potential problem, we applied CBF measurement, a simple and physiologically meaningful way to assess the severity of ischemia in different brain regions. Our data show that the ischemic regions demarcated by TTC staining defect indeed suffer severe CBF reduction (~90%), which is in good agreement with the general belief that, all other factors being equal, the greater the CBF deficit, the less time it takes for neuronal damage to develop. In the regions with rapid BBB disruption, tissue is found to experience a relatively less severe CBF reduction (~70%), and this CBF deficit is not severe enough to rapidly cause neuronal damage to an extent that can be recognized by TTC staining. We and others have previously demonstrated "focal no-reflow" phenomenon in the ischemic territory after MCAO and reperfusion due to microvascular obstruction (del Zoppo and Mabuchi, 2003; Liu et al., 2002). Therefore, there is a possibility that no tracer leakage in severely hypoperfused tissue is due to lack of postischemic reperfusion, which limits tracer delivery to these ischemic regions. This possibility is excluded based on the following considerations: 1) all 2-h MCAO rats consistently showed tracer leakage in the ischemic ventromedial striatum and/or the preoptic area, but no leakage in ischemic cortex; 2) cortical BBB leakage was seen in approximately half of the 3-h MCAO rats (see below); 3) particularly for this purpose, we did CBF measurement in 4 rats right after 2-h MCAO, MRI perfusion map showed good reperfusion in the MCA territory (data not shown). Taken together, although our data are not able to precisely tell the damaging degree of the ischemic tissue positively stained with TTC, these results clearly suggest that BBB damage develops faster in brain regions that suffer from moderately severe ischemia. Currently, we don't know the mechanisms underlying this unexpected finding, we speculate that moderately-reduced CBF may trigger reperfusion-like damaging events such as increased reactive oxygen species generations in hypoperfused tissue to accelerate BBB damage (Abbruscato and Davis, 1999; Kahles et al., 2007). Future studies are warranted to test this hypothesis.

It is an unexpected finding that the two different sized dextrans showed almost identical leakage pattern after 2-h MCAO. In an earlier study, 2000 kDa dextran showed a significant smaller leakage area than 77 kDa dextran after 3-h MCAO with 3 h, but not 21 h, of reperfusion (Nagaraja et al., 2008). From these data, we speculate that ischemia-induced BBB opening may present as an "all-or-none" phenomenon, while the pore size of reperfusion-associated BBB opening may increase with time. This assumption seems not to be supported by an earlier observation that the leakage area of IgG (~150 kDa) greatly exceeded the area of 2000 kDa dextran leakage after 1, 2, 4 and 8 h of MCAO with 30 min reperfusion (Chen et al., 2009). However, in that study, dextran and IgG were injected 20 min prior to ischemia induction. The prolonged presence of these tracers within the cerebrovasculature may lead to additional tracer extravasation due to the potential toxicity of dextran (Michalski et al., 2010) and the capability of IgG to cross intact BBB, though at a low rate (Poduslo et al., 1994).

Although 2-h and 3-h MCAO readily induce tissue infarction evidenced by TTC staining defect in the cortical tissue, cortical BBB leakage is only seen in some (9 out of 16, Figs. 1 and 6) 3-h MCAO rats, and is less severe than subcortical leakage (spots *versus* patches). Interestingly, this severity difference in BBB damage seems to be continued during reperfusion because greater subcortical BBB damage has been reported than cortical BBB damage after 3-h MCAO with 3

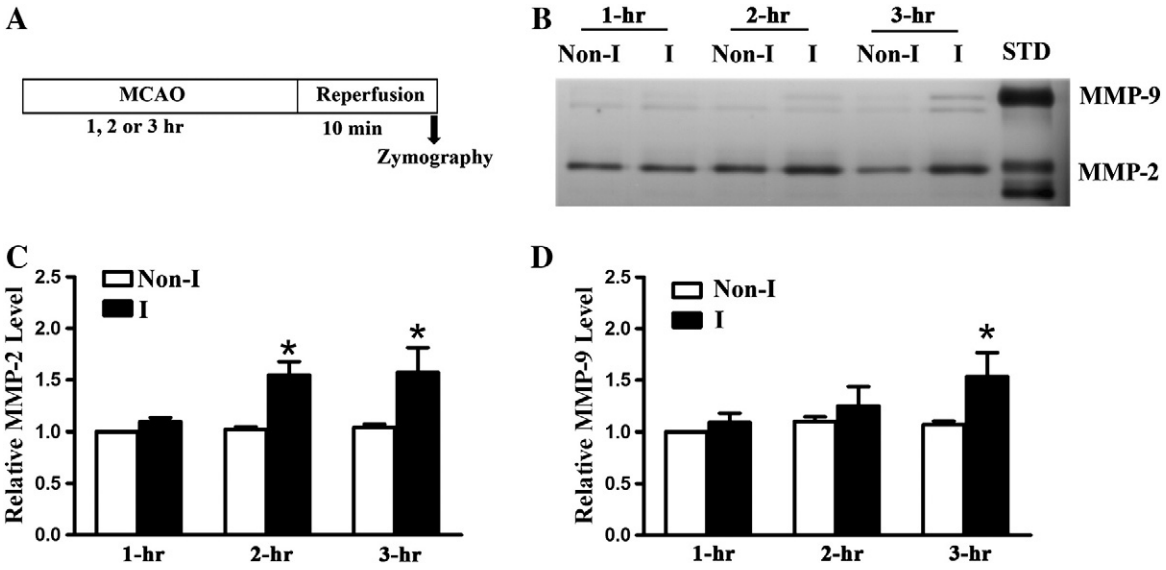

Fig. 4. MMP-2/9 induction in ischemic brain tissue after 1, 2 and 3 h of MCAO. A, Diagram of the experimental procedure. B, Representative gelatin zymogram showing MMP-2/9 levels in the nonischemic (Non-I) and ischemic (I) hemispheric tissue. MMP-2 bands were much stronger than MMP-9 bands on zymogram gels. STD is a mixture of standard MMP-2/9. The relative band intensity of MMP-2 (C) and MMP-9 (D) was quantified. A significant increase was observed for MMP-2 in the ischemic tissue after 2-h MCAO, (*$P<0.05$ *versus* Non-I, n = 6), which was not further increased with the prolongation of ischemic duration to 3 h. MMP-9 responded to MCAO in a slightly delayed pace as its significant increase was observed after 3-h MCAO. (*$P<0.05$ *versus* Non-I, n = 6). No significant changes were observed for both MMP-2 and 9 after 1-h MCAO ($P>0.05$, n = 6). Data were expressed as mean ± SEM.

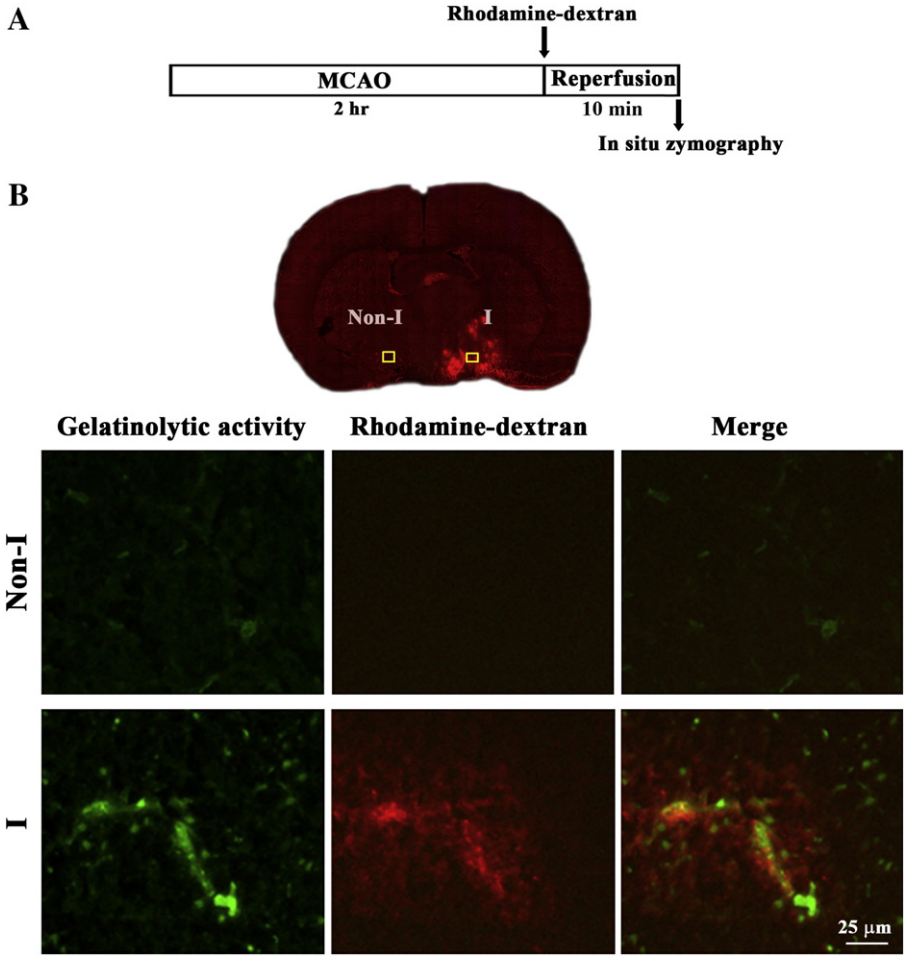

Fig. 5. Colocalization of increased gelatinolytic activity with dextran extravasation in the ischemic brain after 2-h MCAO. A, Diagram of the experimental procedure. B, Top: Rhodamine-dextran leakage (red) was seen in the ischemic preoptic area after 2-h MCAO. After *in situ* zymography procedure, ischemic region (I) with dextran leakage (right square) and its corresponding tissue (left square) in the nonischemic hemisphere (Non-I) were chosen for microscopic observation. Bottom: fluorescent micrographs showed increased gelatinolytic activity of MMP-2/9 along an ischemic microvessel (bright green fluorescence), where dextran leakage concurrently occurred. Spotted distribution of increased gelatinolytic activity was also seen in the leaky area. No dextran leakage and weak gelatinolytic activity were seen in the corresponding region of the nonischemic hemisphere (n = 3). (For interpretation of the references to color in this figure legend, the reader is referred to the web version of this article.)

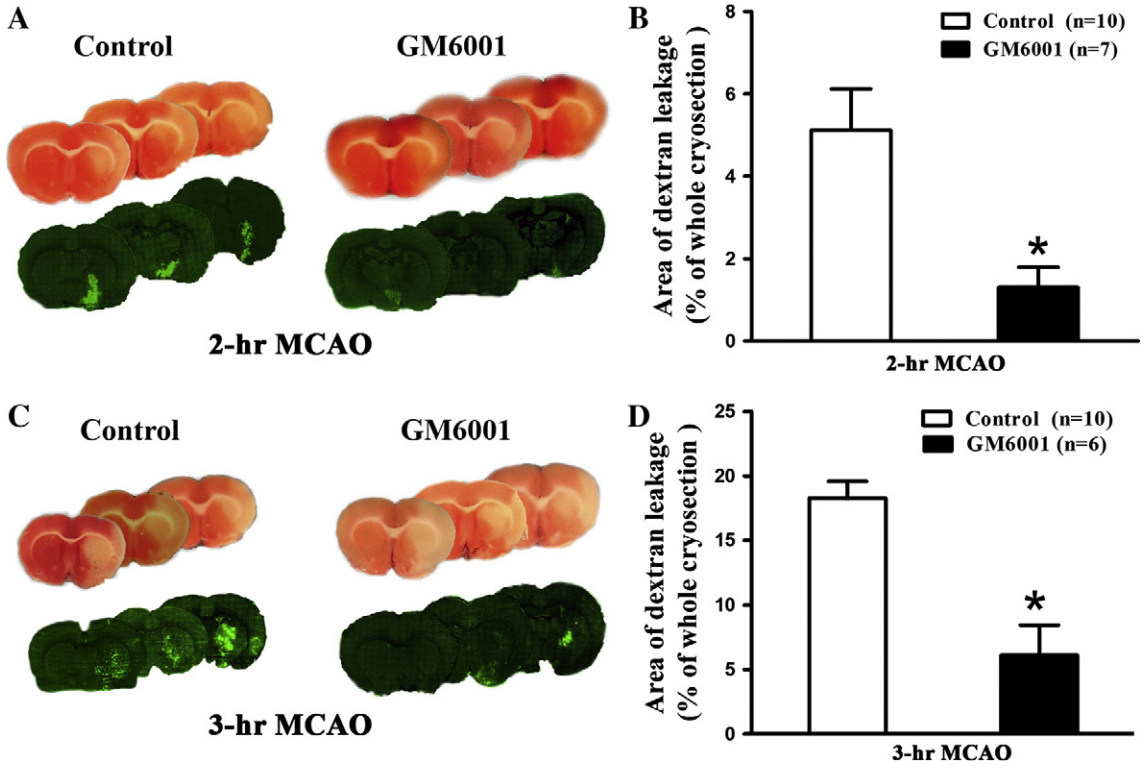

Fig. 6. Pretreatment with MMP inhibitor GM6001 attenuated dextran extravasation induced by 2-h and 3-h MCAO. GM6001 or its negative control (Control) was given to rats 10 min before MACO onset. For each rat, one 1-mm-thick brain slice and one adjacent 20-μm-thick cryosection were prepared for TTC staining and microscopic observation, respectively. A and C, Representative TTC-stained brain slices and fluorescent micrographs revealed tissue infarction and FITC-dextran extravasation in the ischemic hemisphere of GM6001- or Control-treated 2-h or 3-h MCAO rats. B and D, The leaky area was quantified and expressed as percentage of the whole cryosection. Pretreatment with GM6001 significantly reduced FITC-dextran leakage induced by 2-h (B) and 3-h (D) MCAO (*$P<0.05$ *versus* Control). Data were expressed as mean ± SEM.

or 21 h of reperfusion (Hamann et al., 2002; Nagaraja et al., 2008, 2011). Looking more closely at the spatial distribution of ischemia-induced BBB damage, we noticed that the subcortical tissue of the central slice extending from 0.0 to −2.0 mm relative to the bregma experienced the most severe BBB damage, reflected by high density and large patches of tracer leakage. By coincidence, we have previously shown that tPA-associated macroscopic hemorrhage also maximized in the subcortical tissue of the same brain region after 5-h MCAO with 19-h reperfusion (Liu et al., 2009a). In another recent study, Sun et al. also showed that the ischemic striatal tissue with compromised BBB at 2.5 h after MACO underwent hemorrhagic transformation at 24 h after MCAO (Sun et al., 2010). These observations raise an important possibility that the severity of BBB damage set by early ischemia is a key factor determining whether the ischemic tissue will undergo hemorrhagic transformation following thrombolytic reperfusion.

The gelatinases MMP-2/9 are well known mediators for reperfusion-associated BBB damage (Kamada et al., 2007; Romanic et al., 1998; Wang et al., 2003; Yang et al., 2007). Our data support an important role of MMP-2 in early ischemic BBB damage because (1) MMP-2 shows much stronger band on zymogram gels than MMP-9, and the temporal profile of MMP-2 increase (≥2-h MCAO) matches well with the time course of ischemic BBB damage; (2) topographically, BBB damage occurs in the ischemic brain tissue with increased gelatinolytic activity; and (3) pretreatment with broad-spectrum MMP inhibitor GM6001 significantly reduced early ischemic BBB damage. It is not surprising to see a weak band for MMP-9 because, as an inflammatory molecule, MMP-9 increase often occurs at relative late stroke stages after the activation of inflammatory responses (McColl et al., 2008; Yang et al., 2007). Activation of gelatinases has been shown to mediate ischemic neuronal cell death after cerebral ischemia and reperfusion (Gu et al., 2005; Yang et al., 2010), however, this may not be the case for early ischemic neuronal injury because pretreatment with GM6001 appears not to affect the size of TTC staining defect after 2 and 3 h of MCAO (Fig. 6, quantitative data not shown). Worthy of note, our data do not exclude the possibility that other MMP family members may also contribute to early ischemic BBB damage. Future studies are required to define the cellular sources of gelatinases in such early ischemic stroke stages.

Altogether, these data suggest that MCAO induces different topographic distributions of tissue infarction and BBB damage in early ischemic stroke stages. Ischemic BBB damage seems to first occur in the ischemic tissue that suffers relatively less severe hypoperfusion. In addition, MMP-2 plays an important role in this early ischemic BBB damage.

Acknowledgments

Images were generated in the University of New Mexico & Cancer Center Fluorescence Microscopy Shared Resource, funded as detailed on: http://hsc.unm.edu/crtc/microscopy/Facility.html. This work was supported by grants from National Institutes of Health (P20 RR15636 and R01 AG031725), and American Heart Association (10BGIA3190010).

References

Abbruscato, T.J., Davis, T.P., 1999. Protein expression of brain endothelial cell E-cadherin after hypoxia/aglycemia: influence of astrocyte contact. Brain Res. 842, 277–286.
Bang, O.Y., Buck, B.H., Saver, J.L., Alger, J.R., Yoon, S.R., Starkman, S., Ovbiagele, B., Kim, D., Ali, L.K., Sanossian, N., Jahan, R., Duckwiler, G.R., Vinuela, F., Salamon, N., Villablanca, J.P., Liebeskind, D.S., 2007. Prediction of hemorrhagic transformation after recanalization therapy using T2*-permeability magnetic resonance imaging. Ann. Neurol. 62, 170–176.
Bederson, J.B., Pitts, L.H., Germano, S.M., Nishimura, M.C., Davis, R.L., Bartkowski, H.M., 1986. Evaluation of 2,3,5-triphenyltetrazolium chloride as a stain for detection and quantification of experimental cerebral infarction in rats. Stroke 17, 1304–1308.

Belayev, L., Busto, R., Zhao, W., Ginsberg, M.D., 1996. Quantitative evaluation of blood–brain barrier permeability following middle cerebral artery occlusion in rats. Brain Res. 739, 88–96.

Benchenane, K., Berezowski, V., Ali, C., Fernandez-Monreal, M., Lopez-Atalaya, J.P., Brillault, J., Chuquet, J., Nouvelot, A., MacKenzie, E.T., Bu, G., Cecchelli, R., Touzani, O., Vivien, D., 2005a. Tissue-type plasminogen activator crosses the intact blood–brain barrier by low-density lipoprotein receptor-related protein-mediated transcytosis. Circulation 111, 2241–2249.

Benchenane, K., Berezowski, V., Fernandez-Monreal, M., Brillault, J., Valable, S., Dehouck, M.P., Cecchelli, R., Vivien, D., Touzani, O., Ali, C., 2005b. Oxygen glucose deprivation switches the transport of tPA across the blood–brain barrier from an LRP-dependent to an increased LRP-independent process. Stroke 36, 1065–1070.

Betz, A.L., Coester, H.C., 1990. Effect of steroids on edema and sodium uptake of the brain during focal ischemia in rats. Stroke 21, 1199–1204.

Chen, B., Friedman, B., Cheng, Q., Tsai, P., Schim, E., Kleinfeld, D., Lyden, P.D., 2009. Severe blood–brain barrier disruption and surrounding tissue injury. Stroke 40, e666–e674.

del Zoppo, G.J., Mabuchi, T., 2003. Cerebral microvessel responses to focal ischemia. J. Cereb. Blood Flow Metab. 23, 879–894.

del Zoppo, G.J., von Kummer, R., Hamann, G.F., 1998. Ischaemic damage of brain microvessels: inherent risks for thrombolytic treatment in stroke. J. Neurol. Neurosurg. Psychiatry 65, 1–9.

Dewar, D., Underhill, S.M., Goldberg, M.P., 2003. Oligodendrocytes and ischemic brain injury. J. Cereb. Blood Flow Metab. 23, 263–274.

DiNapoli, V.A., Huber, J.D., Houser, K., Li, X., Rosen, C.L., 2008. Early disruptions of the blood–brain barrier may contribute to exacerbated neuronal damage and prolonged functional recovery following stroke in aged rats. Neurobiol. Aging 29, 753–764.

Foley, L.M., Hitchens, T.K., Barbe, B., Zhang, F., Ho, C., Rao, G.R., Nemoto, E.M., 2010. Quantitative temporal profiles of penumbra and infarction during permanent middle cerebral artery occlusion in rats. Transl. Stroke Res. 1, 220–229.

Gerriets, T., Walberer, M., Ritschel, N., Tschernatsch, M., Mueller, C., Bachmann, G., Schoenburg, M., Kaps, M., Nedelmann, M., 2009. Edema formation in the hyperacute phase of ischemic stroke. Laboratory investigation. J. Neurosurg. 111, 1036–1042.

Gu, Z., Cui, J., Brown, S., Fridman, R., Mobashery, S., Strongin, A.Y., Lipton, S.A., 2005. A highly specific inhibitor of matrix metalloproteinase-9 rescues laminin from proteolysis and neurons from apoptosis in transient focal cerebral ischemia. J. Neurosci. 25, 6401–6408.

Hamann, G.F., Liebetrau, M., Martens, H., Burggraf, D., Kloss, C.U., Bultemeier, G., Wunderlich, N., Jager, G., Pfefferkorn, T., 2002. Microvascular basal lamina injury after experimental focal cerebral ischemia and reperfusion in the rat. J. Cereb. Blood Flow Metab. 22, 526–533.

Hjort, N., Wu, O., Ashkanian, M., Solling, C., Mouridsen, K., Christensen, S., Gyldensted, C., Andersen, G., Ostergaard, L., 2008. MRI detection of early blood–brain barrier disruption: parenchymal enhancement predicts focal hemorrhagic transformation after thrombolysis. Stroke 39, 1025–1028.

Hom, J., Dankbaar, J.W., Soares, B.P., Schneider, T., Cheng, S.C., Bredno, J., Lau, B.C., Smith, W., Dillon, W.P., Wintermark, M., 2011. Blood–brain barrier permeability assessed by perfusion CT predicts symptomatic hemorrhagic transformation and malignant edema in acute ischemic stroke. AJNR Am. J. Neuroradiol. 32, 41–48.

Huang, Z.G., Xue, D., Preston, E., Karbalai, H., Buchan, A.M., 1999. Biphasic opening of the blood–brain barrier following transient focal ischemia: effects of hypothermia. Can. J. Neurol. Sci. 26, 298–304.

Kahles, T., Luedike, P., Endres, M., Galla, H.J., Steinmetz, H., Busse, R., Neumann-Haefelin, T., Brandes, R.P., 2007. NADPH oxidase plays a central role in blood–brain barrier damage in experimental stroke. Stroke 38, 3000–3006.

Kamada, H., Yu, F., Nito, C., Chan, P.H., 2007. Influence of hyperglycemia on oxidative stress and matrix metalloproteinase-9 activation after focal cerebral ischemia/reperfusion in rats: relation to blood–brain barrier dysfunction. Stroke 38, 1044–1049.

Kassner, A., Roberts, T.P., Moran, B., Silver, F.L., Mikulis, D.J., 2009. Recombinant tissue plasminogen activator increases blood–brain barrier disruption in acute ischemic stroke: an MR imaging permeability study. AJNR Am. J. Neuroradiol. 30, 1864–1869.

Kuroiwa, T., Ting, P., Martinez, H., Klatzo, I., 1985. The biphasic opening of the blood–brain barrier to proteins following temporary middle cerebral artery occlusion. Acta Neuropathol. (Berl.) 68, 122–129.

Liu, K.J., Rosenberg, G.A., 2005. Matrix metalloproteinases and free radicals in cerebral ischemia. Free Radic. Biol. Med. 39, 71–80.

Liu, S., Connor, J., Peterson, S., Shuttleworth, C.W., Liu, K.J., 2002. Direct visualization of trapped erythrocytes in rat brain after focal ischemia and reperfusion. J. Cereb. Blood Flow Metab. 22, 1222–1230.

Liu, W., Sood, R., Chen, Q., Sakoglu, U., Hendren, J., Cetin, O., Miyake, M., Liu, K.J., 2008. Normobaric hyperoxia inhibits NADPH oxidase-mediated matrix metalloproteinase-9 induction in cerebral microvessels in experimental stroke. J. Neurochem. 107, 1196–1205.

Liu, W., Hendren, J., Qin, X.J., Liu, K.J., 2009a. Normobaric hyperoxia reduces the neurovascular complications associated with delayed tissue plasminogen activator treatment in a rat model of focal cerebral ischemia. Stroke 40, 2526–2531.

Liu, W., Hendren, J., Qin, X.J., Shen, J., Liu, K.J., 2009b. Normobaric hyperoxia attenuates early blood–brain barrier disruption by inhibiting MMP-9-mediated occludin degradation in focal cerebral ischemia. J. Neurochem. 108, 811–820.

Liu, J., Jin, X., Liu, K.J., Liu, W., 2012. Matrix metalloproteinase-2-mediated occludin degradation and caveolin-1-mediated claudin-5 redistribution contribute to blood–brain barrier damage in early ischemic stroke stage. J. Neurosci. 32, 3044–3057.

McColl, B.W., Rothwell, N.J., Allan, S.M., 2008. Systemic inflammation alters the kinetics of cerebrovascular tight junction disruption after experimental stroke in mice. J. Neurosci. 28, 9451–9462.

Menzies, S.A., Betz, A.L., Hoff, J.T., 1993. Contributions of ions and albumin to the formation and resolution of ischemic brain edema. J. Neurosurg. 78, 257–266.

Michalski, D., Grosche, J., Pelz, J., Schneider, D., Weise, C., Bauer, U., Kacza, J., Gartner, U., Hobohm, C., Hartig, W., 2010. A novel quantification of blood–brain barrier damage and histochemical typing after embolic stroke in rats. Brain Res. 1359, 186–200.

Nagaraja, T.N., Keenan, K.A., Fenstermacher, J.D., Knight, R.A., 2008. Acute leakage patterns of fluorescent plasma flow markers after transient focal cerebral ischemia suggest large openings in blood–brain barrier. Microcirculation 15, 1–14.

Nagaraja, T.N., Ewing, J.R., Karki, K., Jacobs, P.E., Divine, G.W., Fenstermacher, J.D., Patlak, C.S., Knight, R.A., 2011. MRI and quantitative autoradiographic studies following bolus injections of unlabeled and (14) C-labeled gadolinium-diethylenetriaminepentaacetic acid in a rat model of stroke yield similar distribution volumes and blood-to-brain influx rate constants. NMR Biomed. 24, 547–558.

Namura, S., Zhu, J., Fink, K., Endres, M., Srinivasan, A., Tomaselli, K.J., Yuan, J., Moskowitz, M.A., 1998. Activation and cleavage of caspase-3 in apoptosis induced by experimental cerebral ischemia. J. Neurosci. 18, 3659–3668.

Poduslo, J.F., Curran, G.L., Berg, C.T., 1994. Macromolecular permeability across the blood–nerve and blood–brain barriers. Proc. Natl. Acad. Sci. U. S. A. 91, 5705–5709.

Qin, Z., Karabiyikoglu, M., Hua, Y., Silbergleit, R., He, Y., Keep, R.F., Xi, G., 2007. Hyperbaric oxygen-induced attenuation of hemorrhagic transformation after experimental focal transient cerebral ischemia. Stroke 38, 1362–1367.

Romanic, A.M., White, R.F., Arleth, A.J., Ohlstein, E.H., Barone, F.C., 1998. Matrix metalloproteinase expression increases after cerebral focal ischemia in rats: inhibition of matrix metalloproteinase-9 reduces infarct size. Stroke 29, 1020–1030.

Strbian, D., Durukan, A., Pitkonen, M., Marinkovic, I., Tatlisumak, E., Pedrono, E., Abo-Ramadan, U., Tatlisumak, T., 2008. The blood–brain barrier is continuously open for several weeks following transient focal cerebral ischemia. Neuroscience 153, 175–181.

Sun, L., Zhou, W., Mueller, C., Sommer, C., Heiland, S., Bauer, A.T., Marti, H.H., Veltkamp, R., 2010. Oxygen therapy reduces secondary hemorrhage after thrombolysis in thromboembolic cerebral ischemia. J. Cereb. Blood Flow Metab. 30, 1651–1660.

Tomita, M., Fukuuchi, Y., 1996. Leukocytes, macrophages and secondary brain damage following cerebral ischemia. Acta Neurochir. Suppl. 66, 32–39.

Vivaldi, M.T., Kloner, R.A., Schoen, F.J., 1985. Triphenyltetrazolium staining of irreversible ischemic injury following coronary artery occlusion in rats. Am. J. Pathol. 121, 522–530.

Wang, X., Lee, S.R., Arai, K., Lee, S.R., Tsuji, K., Rebeck, G.W., Lo, E.H., 2003. Lipoprotein receptor-mediated induction of matrix metalloproteinase by tissue plasminogen activator. Nat. Med. 9, 1313–1317.

Warach, S., Latour, L.L., 2004. Evidence of reperfusion injury, exacerbated by thrombolytic therapy, in human focal brain ischemia using a novel imaging marker of early blood–brain barrier disruption. Stroke 35, 2659–2661.

Williams, D.S., Detre, J.A., Leigh, J.S., Koretsky, A.P., 1992. Magnetic resonance imaging of perfusion using spin inversion of arterial water. Proc. Natl. Acad. Sci. U. S. A. 89, 212–216.

Wu, S., Thornhill, R.E., Chen, S., Rammo, W., Mikulis, D.J., Kassner, A., 2009. Relative recirculation: a fast, model-free surrogate for the measurement of blood–brain barrier permeability and the prediction of hemorrhagic transformation in acute ischemic stroke. Invest. Radiol. 44, 662–668.

Yang, Y., Estrada, E.Y., Thompson, J.F., Liu, W., Rosenberg, G.A., 2007. Matrix metalloproteinase-mediated disruption of tight junction proteins in cerebral vessels is reversed by synthetic matrix metalloproteinase inhibitor in focal ischemia in rat. J. Cereb. Blood Flow Metab. 27, 697–709.

Yang, Y., Candelario-Jalil, E., Thompson, J.F., Cuadrado, E., Estrada, E.Y., Rosell, A., Montaner, J., Rosenberg, G.A., 2010. Increased intranuclear matrix metalloproteinase activity in neurons interferes with oxidative DNA repair in focal cerebral ischemia. J. Neurochem. 112, 134–149.